

April 15, 2006

Structure and magnetism of nanocrystalline exchange-coupled $(\text{Ni}_{0.67}\text{Co}_{0.25}\text{Fe}_{0.08})_{89-x}\text{Zr}_7\text{B}_4\text{Cu}_x$ ($x=0,1$) films

S. Joshi
Northeastern University

S. D. Yoon
Northeastern University

A. Yang
Northeastern University

N. X. Sun
Northeastern University

C. Vittoria
Northeastern University

See next page for additional authors

Recommended Citation

Joshi, S.; Yoon, S. D.; Yang, A.; Sun, N. X.; Vittoria, C.; Harris, V. G.; Goswami, R.; Willard, M.; and Shi, N., "Structure and magnetism of nanocrystalline exchange-coupled $(\text{Ni}_{0.67}\text{Co}_{0.25}\text{Fe}_{0.08})_{89-x}\text{Zr}_7\text{B}_4\text{Cu}_x$ ($x=0,1$) films" (2006). *Electrical and Computer Engineering Faculty Publications*. Paper 127. <http://hdl.handle.net/2047/d20002298>

Author(s)

S. Joshi, S. D. Yoon, A. Yang, N. X. Sun, C. Vittoria, V. G. Harris, R. Goswami, M. Willard, and N. Shi



Structure and magnetism of nanocrystalline exchange-coupled $(\text{Ni}_{0.67}\text{Co}_{0.25}\text{Fe}_{0.08})_{89-x}\text{Zr}_{7}\text{B}_{4}\text{Cu}_x$ ($x = 0, 1$) films

Shashidhar Joshi, Soack Dae Yoon, Aria Yang, Nian X. Sun, Carmine Vittoria et al.

Citation: *J. Appl. Phys.* **99**, 08F115 (2006); doi: 10.1063/1.2176909

View online: <http://dx.doi.org/10.1063/1.2176909>

View Table of Contents: <http://jap.aip.org/resource/1/JAPIAU/v99/i8>

Published by the [American Institute of Physics](#).

Additional information on *J. Appl. Phys.*

Journal Homepage: <http://jap.aip.org/>

Journal Information: http://jap.aip.org/about/about_the_journal

Top downloads: http://jap.aip.org/features/most_downloaded

Information for Authors: <http://jap.aip.org/authors>

ADVERTISEMENT

LakeShore Model 8404 developed with **TOYO Corporation**
NEW AC/DC Hall Effect System Measure mobilities down to 0.001 cm²/V s

Structure and magnetism of nanocrystalline exchange-coupled $(\text{Ni}_{0.67}\text{Co}_{0.25}\text{Fe}_{0.08})_{89-x}\text{Zr}_7\text{B}_4\text{Cu}_x$ ($x=0, 1$) films

Shashidhar Joshi,^{a)} Soack Dae Yoon, Aria Yang, Nian X. Sun, Carmine Vittoria, and Vincent G. Harris

Northeastern University, Boston, Massachusetts 02115

Ramasis Goswami and Matthew Willard

Naval Research Laboratory, Washington, DC 20375

Ning Shi

Hitachi GST, 5600 Cottle Road, San Jose, California 95193

(Presented on 1 November 2005; published online 27 April 2006)

Structural and magnetic characterizations of nanocrystalline films of $(\text{Ni}_{0.67}\text{Co}_{0.25}\text{Fe}_{0.08})_{89-x}\text{Zr}_7\text{B}_4\text{Cu}_x$ ($x=0, 1$) alloys are reported. The films were grown on quartz substrates using pulsed laser deposition from homogeneous targets of the above compositions at substrate temperatures ranging from ambient to 600 °C. Structural properties were measured by x-ray diffraction, atomic force microscopy, and transmission electron microscopy, whereas the magnetic properties were measured by vibrating sample magnetometry and ferromagnetic resonance. The resulting films exist as a two phase alloy with face-centered-cubic metallic grains suspended in an amorphous matrix. For both the $x=1$ and $x=0$ alloys, the softest magnetic properties (coercivity $H_c < 0.5$ Oe, $4\pi M_s \sim 7000$ G) coincided to a deposition at 300 °C in which the fcc grain size (D) was 6–8 nm separated by an amorphous phase of ~ 1 nm. At higher substrate temperatures (T_s) grain size follow a T_s^{-2} dependence, while at lower temperatures the grain size is comparable but the volume of the amorphous matrix is larger and hence the exchange coupling is comparatively weak. A power law relationship is observed between the coercivity and grain size with $H_c \propto D^3$. These results are consistent with the results of Suzuki *et al.* [J. Magn. Magn. Mater. **177–181**, 949 (1998)] for the nanostructure being dominated by a uniaxial anisotropy. © 2006 American Institute of Physics. [DOI: [10.1063/1.2176909](https://doi.org/10.1063/1.2176909)]

I. INTRODUCTION

With the increasing demand for smaller passive components that operate at higher frequencies and temperatures, the electronics industry is in need of improved alloys for use in thin film inductors. Specifically, these materials should possess a high permeability, high saturation magnetization, and low coercivity. Ideally, they should also have small eddy current losses at the target frequency. To this end, we have prepared and studied the dc and rf magnetic properties of nanocrystalline exchange-coupled alloy (NECA) films. The alloys we have chosen have attractive properties when prepared as bulk ribbons¹ where they were characterized to have a nanograined microstructure in which fcc metallic crystallites were imbedded within an amorphous matrix. Previous studies have shown them to have low coercivity, low core losses, low magnetostriction, moderate saturation magnetization, and high permeability. In this paper, we present the structural and magnetic properties of $(\text{Ni}_{0.67}\text{Co}_{0.25}\text{Fe}_{0.08})_{88}\text{Zr}_7\text{B}_4\text{Cu}_1$ and $(\text{Ni}_{0.67}\text{Co}_{0.25}\text{Fe}_{0.08})_{89}\text{Zr}_7\text{B}_4$ films, which demonstrate their potential for high frequency applications.

Nanocrystalline soft magnetic materials were developed by Yoshizawa *et al.* at Hitachi metals.² One of these alloys had the composition $\text{Fe}_{73.5}\text{Si}_{13.5}\text{Nb}_3\text{B}_9\text{Cu}_1$ which today goes by the trade name Finemet. The addition of 1 at. % of Cu

was shown by Ayers *et al.* to be of prime importance for the nucleation and growth of the nanocrystalline metallic phase.³ However, its role in other NECAs remains unclear. Herzer⁴ observed a power law relationship between the coercivity and the grain size ($H_c \propto D^6$) of nanostructured soft magnetic alloys and subsequently proposed a random anisotropy model that explains the soft magnetic properties. This theory is widely accepted today. In 1998, Suzuki *et al.*⁵ demonstrated that for systems that possess a strong uniaxial anisotropy, i.e., much greater than the random magnetocrystalline anisotropy, the D^6 law did not hold but instead the correlation was D^3 .

In the present study we find that for films having a well-defined uniaxial anisotropy a power law relationship is observed with $H_c \propto D^3$. These results are consistent with those of Suzuki *et al.* and that the nanostructure is dominated by a uniaxial anisotropy.

II. EXPERIMENTAL PROCEDURE

Films, ranging in thickness from 200 to 300 nm, were deposited onto fused quartz substrates by pulsed laser deposition (PLD) of alloy targets. Deposition of these films was carried out at a constant laser energy of 400 mJ ($\lambda = 248$ nm) and at 10 mTorr of argon gas. Isothermal substrate temperatures (T_s) were controlled during growth, between room temperature and 600 °C.

^{a)}Electronic mail: sjoshi@coe.neu.edu

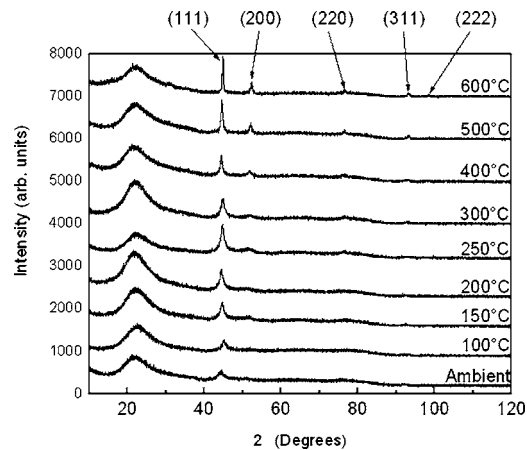


FIG. 1. X-ray diffraction pattern for Cu-containing samples prepared under isothermal substrate temperatures as indicated. The Miller indices of all diffraction peaks are indexed to a fcc metallic phase.

Structural properties were determined by x-ray diffraction (XRD), atomic force microscopy (AFM), and transmission electron microscopy (TEM). The microstructure was examined on ion milled samples using a Philips CM-30 (300 keV) for conventional TEM and a JEOL 2010 (200 keV) for high resolution TEM. Lattice parameters of the nanocrystalline phase were deduced from the XRD patterns ($\text{Cu } K\alpha$) and grain size was determined by Scherrer analysis.⁶ Images of the film nanostructure and microstructure were observed by traditional and high resolution TEMs. Surface morphology was determined by AFM in tapping mode.

Magnetic properties such as coercivity, anisotropy fields, and remanent and saturation magnetizations were determined from room temperature hysteresis loops collected using a vibrating sample magnetometer (VSM) with the applied magnetic field aligned along both the in-plane easy and hard magnetic axes. An angular scan was performed to identify in-plane easy and hard axes. Microwave properties for the films were measured in the H plane of a shorted waveguide technique operating in the TE_{10} mode. Room temperature ferromagnetic resonance (FMR) spectra were taken in the $K\alpha$ -band frequency range using the differential power absorption technique with a HP8690B Sweep Oscillator as the rf source and a lock-in amplifier for detection of the absorption signal.

III. RESULTS AND DISCUSSION

A. Structure and morphology

Figure 1 illustrates the θ - 2θ diffraction patterns of films deposited at different substrate temperatures. The Bragg peaks were indexed, indicating primary crystallites of a face-centered-cubic (fcc) phase. It is noteworthy that the film grown at ambient temperature shows a broad (111) peak indicating the presence of a nanocrystalline phase. This is supported by high resolution TEM (HRTEM) images showing 6 nm diameter grains separated by 2–5 nm of amorphous phase. At higher substrate temperatures, the number and the volume fraction of crystallites increase at the expense of the amorphous matrix. For $T_s \leq 300$ °C, the grain size remains

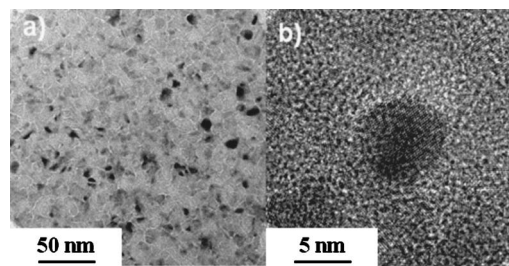


FIG. 2. (a) TEM image of the Cu-containing sample grown at a $T_s = 300$ °C. The amorphous phase appears as white in the image between the grains. (b) HRTEM image of 7 nm grains in an amorphous matrix corresponding to the sample grown under ambient conditions.

10 ± 2 nm in diameter with the best magnetic properties at $T_s = 300$ °C (and grain size 7.5 ± 0.5 nm). The grains increase in size at higher T_s , roughly following a T^2 dependence. The lattice parameter does not change within the uncertainty of the measurements for values of $T_s \leq 300$ °C; however, at higher substrate temperatures there appears to be a trend towards reduced values from 0.355 nm (300 °C) to 0.349 ± 0.001 nm (600 °C) as determined by XRD. The phase, grain size, and lattice parameter are nearly the same as that found in Ref. 1 for the bulk equivalent alloys.

Figure 2(a) shows TEM images for the film deposited at $T_s = 300$ °C with grains of around 6–8 nm in diameter surrounded by a (white) amorphous matrix that is < 1 nm in thickness. A HRTEM image is shown in Fig. 2(b), depicting grains of 5–7 nm diameter separated by an amorphous phase. TEM micrographs for the sample with $T_s = 600$ °C indicate a bimodal distribution of grain sizes with both fcc and Zr intermetallic forming. The larger fcc grains have an average diameter of a few hundred nanometers and the smaller fcc and Zr intermetallic grains have an average grain diameter near 30 nm. This is consistent with the reduction of grain size found by XRD, since many of the nanocrystalline materials tend to have dilated lattice parameters (compared to bulk values). The AFM images (not shown) illustrate a change in topography of the films with increasing substrate temperature. The mean roughness and average height of the films increase with the increase in substrate temperature, closely following trends in grain size determined by XRD and TEM. The $T_s = 300$ °C sample had the lowest value of surface roughness at < 2 nm (rms).

B. dc and microwave magnetic properties

Hysteresis loops were obtained with applied magnetic fields aligned in plane, but in two orientations, along the magnetic easy and hard axes for all samples. The in-plane easy and hard axes were determined by measuring the angular dependence of the remanent magnetization at angles of 0° – 180° . From these data coercivity, anisotropy fields, remanence, and saturation magnetization values were measured. We speculate that the presence of an in-plane uniaxial anisotropy may be due to a pair-order anisotropy occurring as a result of the dynamics of film growth.⁷ Figure 3 shows the hysteresis loops for the $T_s = 300$ °C sample showing very soft magnetic properties (e.g., $H_c < 0.5$ Oe). Coercivity was found to remain nearly constant at 0.5 Oe for films deposited

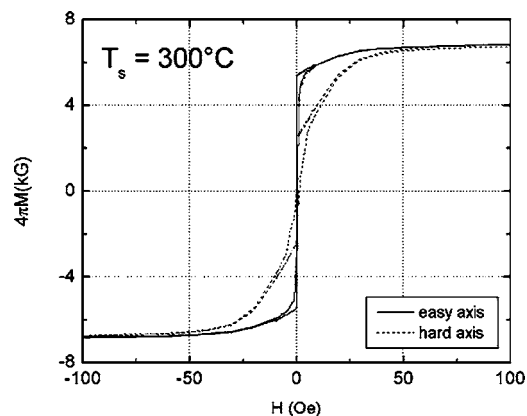


FIG. 3. Hysteresis loops collected from the Cu-containing sample for $T_s = 300$ °C for the applied magnetic field aligned along the in-plane easy and hard axes. The loop squareness for the hard direction is near 0.5, signaling the onset of long range uniaxial anisotropy.

at $T_s \leq 300$ °C and increased dramatically at higher T_s with grain coarsening. The magnetization for films deposited at $T_s \leq 400$ °C remains constant but was reduced at higher substrate temperatures. This reduction in magnetization was attributed to the formation of a surface oxide. Although the XRD does not show signs of this, the color of the film surface appears as a matted gray at $T_s > 400$ °C.

FMR measurements were performed to determine the microwave properties on the films of $(\text{Ni}_{0.67}\text{Co}_{0.25}\text{Fe}_{0.08})_{89-x}\text{Zr}_7\text{B}_4\text{Cu}_x$ where $x=1$. FMR linewidths (ΔH) were carefully measured as a function of frequency for the films deposited at $T_s=300$ °C. There were no significant differences in ΔH vs f in which ΔH remained constant over the frequency range of 27–40 GHz. The lowest ΔH was measured to be 190 Oe at 28 GHz. The Lande spectroscopic splitting factor (g) was deduced from the relation between resonant frequencies versus resonance field to be 2.21. This value is similar to the value for elemental Ni or Co ($g=2.21$) compared to the value for Fe ($g=2.1$).

C. Coercivity, grain size, and the effect of Cu

A comparison of the structural and magnetic properties of the films for both alloys ($x=0,1$) deposited under the same conditions was performed to determine the role of Cu in the evolution of the thin film nanostructure. The structural and magnetic properties of the film samples for $x=0$ and 1 are largely the same for low temperature depositions (i.e., $T_s \leq 250$ °C). One exception is that the $x=0$ alloys deposited at 300 °C experienced an increase in grain size and coercivity, indicating that the onset of grain coarsening occurred at lower temperatures.

Figure 4 is a plot of H_c vs D for both $x=0$ and $x=1$ alloy films. For both alloys we observe a power law dependence near D^3 . This is in agreement with Suzuki *et al.*⁵ who demonstrated a deviation from D^6 to D^3 for samples that possess a long range uniaxial anisotropy (LRUA) energy. This is also seen in the hysteresis loop of Fig. 3 in which the loop squareness (M_r/M_s) is near 0.5. Herzer has suggested that the reduction of the loop squareness to 0.5 signals the transition from a random magnetic anisotropy (RMA) dominated to a LRUA dominated system.⁸ We have found these films to

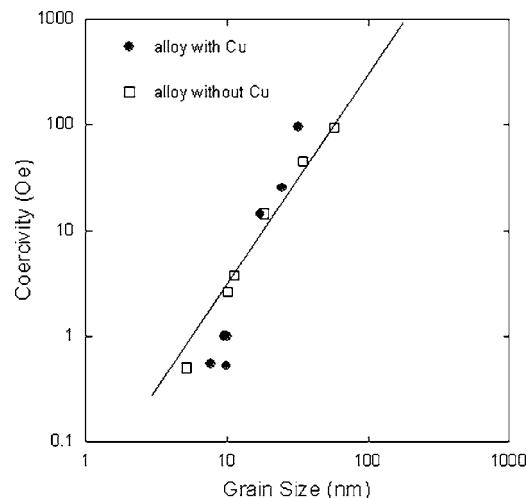


FIG. 4. Coercivity vs grain size illustrating a power law dependence for samples with and without Cu. The line shows a D^3 dependence that is expected for nanocrystalline soft magnetic thin films with an in-plane uniaxial anisotropy.

possess a strong in-plane uniaxial anisotropy, and therefore this result is consistent with the results of Ref. 5. The bimodal grain size distribution for the sample with $T_s=600$ °C indicates that the largest grains (i.e., >50 nm) remain in the RMA dominant region.

IV. CONCLUSIONS

Structural and magnetic characterizations of nanocrystalline films of $(\text{Ni}_{0.67}\text{Co}_{0.25}\text{Fe}_{0.08})_{89-x}\text{Zr}_7\text{B}_4\text{Cu}_x$ ($x=0,1$) alloys are reported. The films were grown on quartz substrates using pulsed laser deposition from homogeneous targets of the above compositions at substrate temperatures ranging from ambient to 600 °C. The resulting films exist as a two phase alloy with face-centered-cubic metallic grains suspended in an amorphous matrix (with additional phases forming at elevated T_s). For both the $x=1$ and $x=0$ alloys, the softest magnetic properties (coercivity $H_c < 0.5$ Oe, $4\pi M_s \sim 7000$ G) coincided to a deposition at 300 °C in which the fcc grain size (D) was 6–8 nm separated by an amorphous phase of ~ 1 nm. A power law relationship between the coercivity and grain size was observed with coercivity exhibiting a near D^3 dependency. These results are consistent with the nanostructure being dominated by long range uniaxial anisotropy.

¹M. A. Willard, J. C. Claassen, R. M. Stroud, T. L. Francavilla, and V. G. Harris, IEEE Trans. Magn. **38** (2002).

²Y. Yoshizawa, S. Oguma, and K. Yamauchi, J. Appl. Phys. **64**, 6044 (1998).

³J. D. Ayers, V. G. Harris, J. A. Sprague, W. T. Elam, and H. N. Jones, Acta Mater. **46**, 1861 (1998); J. D. Ayers, V. G. Harris, J. C. Sprague, W. T. Elam, and H. N. Jones, Nanostruct. Mater. **9**, 391 (1997); J. D. Ayers, V. G. Harris, J. C. Sprague, and W. T. Elam, Appl. Phys. Lett. **64**, 974 (1994).

⁴G. Herzer, IEEE Trans. Magn. **26**, 1397 (1990).

⁵K. Suzuki, G. Herzer, and J. M. Cadogan, J. Magn. Magn. Mater. **177–181**, 949 (1998).

⁶B. D. Cullity, *Elements of X-ray Diffraction*, 2nd ed. (Addison-Wesley, Reading, MA, 1978), p. 102.

⁷V. G. Harris and T. Pokhil, Phys. Rev. Lett. **87**, 067207 (2001).

⁸G. Herzer, J. Magn. Magn. Mater. **157–158**, 133 (1996).